energy&fuels

Article

pubs.acs.org/EF

Insights into the Mechanism of Wettability Alteration by Low-Salinity Flooding (LSF) in Carbonates

Hassan Mahani,*[,†] Arsene Levy Keya,[†] Steffen Berg,[†] Willem-Bart Bartels,[‡] Ramez Nasralla,[†] and William R. Rossen[§]

[†]Shell Global Solutions International B.V., 2288 GS Rijswijk, Netherlands

[‡]University of Utrecht, 3512 JE Utrecht, Netherlands

[§]Delft University of Technology, 2628 CN Delft, Netherlands

Supporting Information

ABSTRACT: The low-salinity effect (LSE) in carbonate rock has been less explored in comparison to sandstone rock. Laboratory experiments have shown that brine composition and (somewhat reduced) salinity can have a positive impact on oil recovery in carbonates. However, the mechanism leading to improved oil recovery in carbonate rock is not well understood. Several studies showed that a positive low-salinity flooding (LSF) effect might be associated with dissolution of rock; however, because of equilibration, dissolution may not contribute at reservoir scale, which would make LSF for carbonate rock less attractive for field applications. This raises now the question whether calcite dissolution is the primary mechanism of the LSF effect. In this paper, we aim to first demonstrate the positive response of carbonate rock to low salinity and then to gain insight into the underlying mechanism(s) specific to carbonate rock. We followed a similar methodology as in sandstone rock [Mahani, H.; Berg, S.; Ilic, D.; Bartels, W.-B.; Joekar-Niasar, V. Kinetics of low-salinity-flooding effect. *SPE J.* **2015**, *20* (1), 8−20, DOI: 10.1021/ef5023847] using a model system comprised of carbonate surfaces obtained from crushed carbonate rocks. Wettability alteration upon exposure to low-salinity brine was examined by continuous monitoring of the contact angle. Furthermore, the effective surface charge at oil−water and water−rock interfaces was quantified via ζ-potential measurements. Mineral dissolution was addressed both experimentally and with geochemical modeling using PHREEQC. Two carbonate rocks with different mineralogy were investigated: limestone and Silurian dolomite. Four types of brines were used: high-salinity formation water (FW), seawater (SW), 25× diluted seawater (25dSW), and 25× diluted seawater equilibrated with calcite (25dSWEQ). It was observed that, by switching from FW to SW, 25dSW, and 25dSWEQ, the limestone surface became less oil-wet. The results with SW and 25dSWEQ suggest that the LSE occurs even in the absence of mineral dissolution, because no dissolution is expected in SW and none in 25dSWEQ. The wettability alteration to a less oil-wetting state by low salinity is consistent with the ζ-potential data of limestone, indicating that, at lower salinities, the charges at the limestone−brine interface become more negative, indicative of a weaker electrostatic adhesion between the oil−brine and rock−brine interfaces, thus recession of the three-phase contact line. In comparison to limestone, a smaller contact angle reduction was observed with dolomite. This is again consistent with the ζ-potential of dolomite, generally showing more positive charges at higher salinities and less decrease at lower salinities. This implies that oil detachment from the dolomite surface requires a larger reduction of adhesion forces at the contact line than limestone. Our study concludes that surface charge change is likely to be the primary mechanism, which means that there is a positive LSE in carbonates without mineral dissolution.

INTRODUCTION

Numerous laboratory and field experiments[1−18] have shown that oil recovery from clay-rich sandstone can be improved in many cases by lowering the total salinity and divalent content of the injected water. It is envisaged that the same concept can be extended to carbonate rocks. However, the low-salinity effect (LSE) in carbonates and the specific underlying mechanisms leading to oil mobilization and recovery have been less explored in comparison to the case for sandstones and are even less understood.

For sandstones, Tang and Morrow[3] pointed out that the effect is inherently linked to the presence of clay minerals and also dependent upon the oil composition, the presence of formation water with a high concentration of divalent cations (Ca^{2+} and Mg^{2+}), and the salinity level of the injected water, preferably below 5000 ppm. However, most carbonate rocks do not contain clay, and if they do, they are at only very low levels. Most carbonate rocks are mainly composed of calcium carbonate (limestone or chalk) either without or with the presence of magnesium (e.g., dolomite). Evaporite rock materials might be present, such as gypsum or anhydrite, that are hydrated and non-hydrated calcium sulfate minerals, respectively.

Bearing in mind this mineralogical difference, low salinity in carbonates cannot necessarily work in exactly the same way as in sandstone. In sandstones, low salinity is recognized as the main parameter driving the effect and is observed usually below a threshold value of 5000−7000 ppm. In carbonates, however,

Received: October 22, 2014
Revised: February 20, 2015
Published: February 20, 2015

DOI: 10.1021/ef5023847
Energy Fuels 2015, 29, 1352−1367

the exact chemical composition of the brine seems to play a more important role than just the overall ionic strength. As will be discussed further below, there are also cases where the LSE has been observed with SW. Its salinity between 30 000 and 45 000 ppm is generally considered beyond the realm of the LSE in sandstones.

In the following, we will review some of the findings that have been published on the low-salinity flooding (LSF) effect in carbonate rock. The studies are summarized in three categories such that different parameters/effects can be separated. Nevertheless, it is realized that they are interlinked and are not totally independent.

Role of Potential Determining Ions (PDIs) on the LSE. Numerous studies indicate that divalent ions, such as Mg^{2+}, Ca^{2+}, and SO_4^{2-} (referred to as PDIs), play an important role in this process, and the lack of response to low salinity in some of the reported cases has been related to the lack of these ions (particularly Mg^{2+} and SO_4^{2-}) in the brine.[19] CO_3^{2-} has also been identified as a PDI in various studies (see, e.g., the study by Heberling et al.[20]); however, its specific role in the context of LSF has not been investigated explicitly as done with Mg^{2+}, Ca^{2+}, and SO_4^{2-}. Contact angle measurements by Chandrasekhar and Mohanty[21] on a calcite surface aged with oil and on a limestone slab by Yousef et al.[22] showed that increasing levels of SO_4^{2-} were effective in wettability alteration from oil-wet (O-W) toward water-wet (W-W). Mg^{2+} and SO_4^{2-} were also recognized as the main PDIs causing a positive effect, albeit only for seawater (SW) and not for formation water (FW). The presence of Ca^{2+} without Mg^{2+} and SO_4^{2-} in SW and FW was found to have a negative effect for both SW and FW. Studies by Tweheyo et al.[23] and Rezaei-Gomari et al.[24] through contact angle measurements on a calcite surface modified with oil and long-chain fatty acids suggests that PDIs become more effective as the temperature increases.

In line with the above results, spontaneous imbibition tests on chalk cores[25−28] confirmed the significance of brine composition and, more specifically, PDIs on wettability of the chalk rock and ultimately on the oil recovery. Zhang and Austad[26] found that an increase of the sulfate ion (SO_4^{2-}) concentration in SW has a positive effect on the oil recovery from the chalk core. An experiment with an increased concentration of Ca^{2+} in SW resulted in a 32% increase in incremental oil recovery after 30 days of imbibition. Further experiments revealed that the rock surface was altered from an oil-wetting state toward a water-wetting state (wettability alteration), yielding higher oil recovery.

Similar observations were made on North Sea chalk under reservoir conditions with sulfate in the imbibing brine,[29] on chalk, limestone, and dolomite core plugs with sulfate-modified low-salinity brine as the imbibing brine,[30] and for sulfate-modified SW as the injection water at reservoir temperature.[21,31−34]

All above-reported studies highlight the importance of Ca^{2+}, Mg^{2+}, and SO_4^{2-} in injection brine. SW typically contains high concentrations of Ca^{2+}, Mg^{2+}, and SO_4^{2}, and that can likely explain why SW often resulted in increased oil recovery. Nevertheless, their concentration in FW is typically very high, and only by selectively reducing or removing Ca^{2+} or Mg^{2+} can the LSE be triggered, as suggested by the results of Gupta et al.[31]

On the relative importance of the PDIs, the study performed by Karoussi and Hamouda[35] shows that Ca^{2+} or SO_4^{2-} alone do not increase oil recovery, which suggests that SO_4^{2-} works only in the presence of Mg^{2+} or Ca^{2+}. In other words, the LSE is the combined effect of PDIs. In the above studies, an increase of SO_4^{2-}/Ca^{2+} has often led to higher oil recovery (or less oil-wetting conditions). From the work reported by Austad et al.[25] and Al-Attar et al.,[36] we note that there could be an optimum concentration of PDI, which leads to the highest LSE.

Effect of Lowering Brine Salinity (e.g., by Dilution) on the LSE. From the published studies, we note that, indeed, in quite a number of cases, the positive LSE can be attributed to the presence of PDIs (at concentrations that are typically high) in the injection water, such as seawater. There are cases where LSE has been observed with low-salinity brine [total dissolved solids (TDS) < 5000 ppm] or diluted SW (TDS ∼ 1000 ppm), wherein the concentration of PDIs is not really significant. This implies that LSE can be alternatively achieved at low TDS (or ionic strength) and the mechanism underlying the LSE does not necessarily involve (or at least is not limited to) PDIs. In other words, the presence of PDIs is not essential in all brines because the LSE has been observed with deionized water and low-salinity brines containing a fairly low concentration of PDIs.

For instance, Chandrasekhar and Mohanty[21] and Zhang and Sarma[32] reported enhancement of spontaneous imbibition and, thereby, oil recovery with low-salinity brine in tertiary recovery and with diluted SW (TDS = 872 ppm) in both tertiary and secondary recovery. Romanuka et al.[30] reported that lowering the ionic strength of brine triggered higher incremental oil recovery in the range of 1−20% from spontaneous imbibition on limestone and dolomite core plugs (except for chalk).

A notable coreflood case by Yousef et al.[37] on carbonate cores showed a stepwise increase in the net incremental oil recovery of approximately 19% by injecting SW and successively diluting by a factor of 100. Alotaibi et al.[38] experienced an 8.6% incremental oil recovery by injecting low-salinity aquifer water, following the injection of FW. Zahid et al.[39] observed a substantial increase in oil recovery in carbonate core plugs with low-salinity water (although only at a high temperature). The coreflood study by Nasralla et al.[40] on limestone cores from Middle Eastern reservoirs demonstrated that diluting SW 10 times can increase oil recovery compared to formation brine injection by altering the rock wettability to a less oil-wetting state. Shehata et al.[34] investigated extreme levels of salinity using Indiana limestone rock. Their coreflooding results indicate that oil recovery can be improved by injection of deionized water after SW injection (and vice versa). While the mechanism was not explicitly investigated, it was hypothesized that it is due to a "sudden" change of brine ionic composition and salinity between different periods of injection.

Effect of Rock Mineralogy/Composition on the LSE. The effect of the carbonate type and mineralogy has not been specifically investigated as much. There exist published results that indicate that LSE depends upon the nature of carbonate rock. For instance, Fernø et al.[41] studied the effect of the sulfate concentration on oil recovery during spontaneous imbibition in different outcrop chalks (Stevns Klint, Rørdal, and Niobrara). Spontaneous imbibition tests showed increasing oil recovery with an increased concentration of sulfate ions only in Stevns Klint chalk, while this effect was not observed in Rørdal and Niobrara. In the study by Romanuka et al.,[30] chalk core plugs did not respond to lowering salinity of the brine, while limestone and dolomite samples did respond.

DOI: 10.1021/ef5023847
Energy Fuels 2015, 29, 1352−1367

Despite the above interesting results, the potential mechanisms explaining the observations have not been addressed sufficiently to make reliable predictions of recovery increases for specific fields.

The current understanding extracted from the literature cited above can be categorized into the following mechanisms.

(1) **Mineral dissolution:** Hiorth et al.[42] proposed this mechanism and established a surface complexation model and correlation between the oil recovery factor and the expected calcite dissolution. Yousef et al.[43] supported this theory by reporting an enhancement in connectivity between micro- and macropores, attributed to mineral dissolution from nuclear magnetic resonance (NMR) data prior and post low-salinity coreflooding tests in carbonates. Some studies[44] propose that anhydrite dissolution from core material (which generates SO_4^{2-} *in situ*) underlies the LSE. However, Pu et al.[45] from their experiments on dolomite rock containing anhydrite concluded that, in addition to anhydrite dissolution, other mechanisms, such as dissolution of other minerals and release of adsorbed organic material, drove the wettability alteration of rock. Romanuka et al.[30] and Nasralla et al.[40] believed that mineral dissolution is not the dominant mechanism for enhanced oil recovery in their experiments.

(2) **Surface charge change:** Most studies agree that the charge at the carbonate rock/brine interface strongly depends upon composition, salinity, and pH of the brine as well as the mineralogy of the rock and the temperature. When a carbonate surface is immersed in a saline solution, the interaction between the ions at the rock surface and the ions present in the brine create an electric double layer (EDL) composed of a dynamically formed diffuse cloud of ions near the rock surface. The interactions between the EDL and a brine−oil interface with polar organic molecules in it are expected to contribute significantly to the overall wettability of carbonate rocks and its alteration by low-salinity waterflooding. On the connection between wettability and surface reactions, Brady et al.[46] and Brady and Krumhansl[47] developed a "surface complexation model", which gives insights into the primary coordination reactions at the rock−brine−oil interfaces, leading to oil adhesion to clay and calcite.

Electrokinetic studies on pure calcite and dolomite crystals have been performed,[20,48−52] which indicate that calcite particles acquire a positive charge below the isoelectric point and a negative charge above the isoelectric point.

Unfortunately, most of the published studies focus on pure calcite or dolomite with indifferent electrolytes, such as NaCl and KCl brines, which are not clearly representative of brines and rocks pertaining to carbonate reservoirs. There are only a few published studies using reservoir rock and brine composition. Alotaibi et al.[53] measured the ζ-potential for outcrop limestone and dolomite rocks with different formation brines containing both di- and monovalent ions. The study shows that lowering the brine salinity leads to a more negatively charged surface, contributing to expansion of the EDL. The addition of specific ions, such as SO_4^{2-}, in brines induced a more negative potential. However, this study did not attempt to connect the behavior of ζ-potential (or electrostatic forces or EDL effect) to the LSE.

The studies conducted by Austad and co-workers[25−27] seem to indicate the importance of surface charge change as a likely LSE mechanism. Their LSE hypothesis is related to the adsorption of PDIs, such as sulfate, onto the rock surface, which triggers desorption of some of the carboxylic groups via their interaction with Mg^{2+} and Ca^{2+} ions. Adsorption of sulfate ions reduces the electrostatic repulsive force that enhances the adsorption of Ca^{2+}/Mg^{2+} ions. This is a plausible mechanism, however limited to the presence of PDIs at sufficiently high concentrations. As will be shown in this paper, the surface charge of carbonate rock can change by diluting the brines, where PDIs are at relatively low concentrations, which suggests a more fundamental process behind the effect than that caused only by PDIs.

(3) A combination of mechanisms 1 and 2 has been proposed by Zaretskiy[54] as well.

(4) **Other mechanisms:** Mechanisms such as *in situ* surfactant generation have also been proposed.[4] However, this requires a high pH (exceeding 10), which rarely occurs in waterflooding and LSF.

From the studies conducted thus far, it is unclear which mechanism dominates, but the focus is on rock dissolution versus surface charge effects. The aim of our work is therefore 2-fold.

The primary aim is to directly, by visual inspection, demonstrate the wettability alteration effect, following low-salinity exposure of a carbonate surface.

The second aim is to establish whether the wettability change is mainly related to dissolution of the carbonate surface or whether there is a different process not requiring dissolution, such as surface charge change (or electrostatic forces).

To address these goals, we used carbonate model surfaces on the oil-droplet scale. The approach follows a similar philosophy and methodology as presented earlier by Mahani et al.[1] on a model system, where the complexity is reduced as much as possible but natural rock and crude oil are used to ensure relevance for the actual field case.

Most of the reported studies probe the LSF effect at the core scale. Experiments at the core scale average over such a large volume of rock with different minerals, which makes it difficult to relate to what happens at the rock surface. Our investigation focuses on two different length scales (as illustrated in Figure 1), namely, the scale of an effective (macroscopic) oil−brine−rock contact angle and the scale of the oil−water and water−rock interface (sub-core and sub-pore). On the scale of the

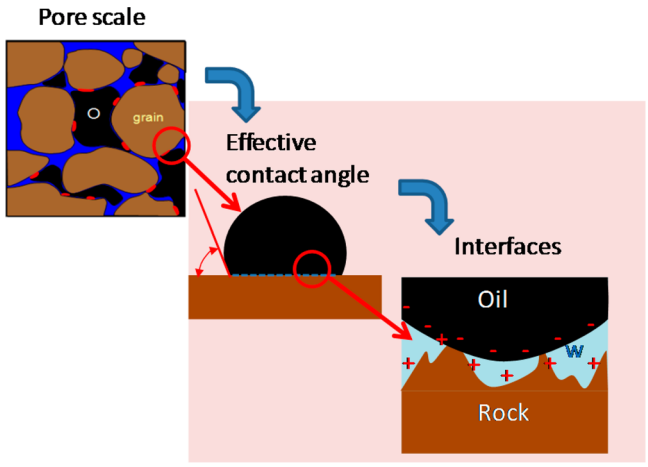

Figure 1. In our study, we concentrate on the scale of the effective (macroscopic) contact angle, where we quantify the effect of LSF by the change in the contact angle and the scale of interfaces, where we quantify the interaction strength of oil and rock via the effective surface charges (ζ-potential).

DOI: 10.1021/ef5023847
Energy Fuels 2015, 29, 1352−1367

Table 1. Mineral Composition of Carbonate Rocks Estimated from XRD (Percentage of Bulk Sample) and Grain Density

		composition					
sample	grain density (g/cm^3)	kaolinite (%)	quartz (%)	K feldspar (%)	plagioclase (%)	calcite (%)	dolomite (%)
limestone	2.844	0	trace	0	0	100	0
Silurian dolomite	2.703	0	1	0	0	0	99

effective contact angle, the wettability alteration is examined by continuously monitoring the contact angle at the interface of oil–brine–rock. On the scale of the oil–water and water–rock interfaces, the effective surface charge is quantified via ζ-potential measurements. On that scale, also, the effect of mineral dissolution is addressed by both experiment and modeling.

MATERIALS AND METHODS

Carbonate Rocks. The types of carbonate material used in this study are limestone and dolomite. Limestone material originates from a core drilled from a carbonate oil reservoir in the Middle East, and the dolomite material is a Silurian dolomite. The mineral composition of the limestone and dolomite cores is presented in Table 1. The samples contain no clay mineral within the detection limits of powder X-ray diffraction (XRD).

The carbonate material is crushed to fabricate the model carbonate surfaces (or patches). The grain sizes of the crushed carbonate are below 45 μm. However, the patches are created using the supernatant part of the suspension, containing the finest grains. Their size falls into the range between 1 and 20 μm as measured by Mastersizer 2000 (Malvern Instruments).

Brine. Synthetic brines are used in this study. The brines are prepared by mixing deionized water and different amounts of pure salts: NaCl, Na_2SO_4, KCl, $NaHCO_3$, $MgCl_2{\cdot}6H_2O$, and $CaCl_2{\cdot}2H_2O$. The FW composition is taken from a Middle Eastern carbonate field. The brines with lower salinity were prepared by diluting SW. 25dSW is seawater diluted 25 times. 25dSWEQ was made by equilibrating 25dSW with limestone particles. Because 25dSW brine is undersaturated, during equilibration with limestone particles, calcium carbonate is dissolved in the brine until reaching saturation, and as a result, pH rises from 7.5 to 9.2.

The composition of the brines is listed in Table 2. The amount of calcite and dolomite dissolution/precipitation in the brines was determined both experimentally using the inductively coupled plasma–mass spectrometry (ICP–MS) method and by geochemical modeling using PHREEQC software, version 3, from the United States Geological Survey (USGS), available at http://wwwbrr.cr.usgs.gov/projects/GWC_coupled/phreeqc/. In Appendix 1 of the Supporting Information, an input file used for calculation of equilibrium composition and pH of brine in the presence of carbonate particles is presented.

Table 2. Chemical Composition of Brines at Ambient Conditions

ion	FW (mg/L)	SW (mg/L)	25dSW (mg/L)	25dSWEQ (mg/L) (composition from PHREEQC)
Na^+	49898	13404	536	536
K^+	0	483	19	19
Mg^{2+}	3248	1618	65	65
Ca^{2+}	14501	508	20	23
Sr^{2+}	0	17	1	1
Cl^-	111812	24141	967	967
SO_4^{2-}	234	3384	135	135
HCO_3^-	162	176	7	12
TDS	179855	43731	1751	1759
ionic strength (mol/L)	3.659	0.869	0.035	0.035
measured pH	6.9	8.0	7.5	9.2

Crude Oil. A crude oil originating from a Middle Eastern carbonate field is used in this study. The oil was centrifuged and filtered through a 1.2 μm Millipore filter and subsequently analyzed for physical and chemical properties (Table 3). The Fourier transform ion cyclotron resonance–mass spectrometer (FTICR–MS) analysis conducted on the oil sample gave a polar compound pattern as expected for regular oil with no indication of contamination.

Table 3. Selected Properties of Oil

acid number (mg of KOH/g)	base number (mg of KOH/g)	asphalthene (g/100 mL)	density (g/cm^3) at 20 °C	viscosity (cP) at 20 °C
0.52	1.00	0.2448	0.8567	20.75

Experimental Setup. The model system experiments are performed using a built-for-purpose experimental setup (shown in Figure 2) for contact angle monitoring and measurement. The experiments are performed on a model substrate (representing the essential elements of a carbonate rock surface), which, in this case, is a microscope glass slide coated with carbonate particles from suspension (analogous to our previous work with clays[1]), on top of which oil drops are attached. The fabrication details are explained further below. The substrate is placed in a glass-windowed cell (flow cell) and is exposed to brines of different salinity under static conditions. Brines are stored in sealed tanks. The flow cell is filled with brines using two Quizix pumps (pump 1 in injection mode and pump 2 in pressure mode), and high pressure can be maintained with the same pumps. The cell is placed in an oven (allowing us to perform experiments at an elevated temperature as well. A high-resolution camera (Nikon Micro NIKKOR 105 mm lens combined with an Imaging Source 72 Series CMOS camera) is installed next to the cell to capture real-time images from individual oil drops through a custom-made interface in LabVIEW software. Contact angle measurements are performed on these images. The camera is placed outside the oven and looks through its window. Inside the oven, a diffuse light source (halogen type) is placed to illuminate the oil drops. The whole setup is mounted on a breadboard to absorb shocks and vibrations.

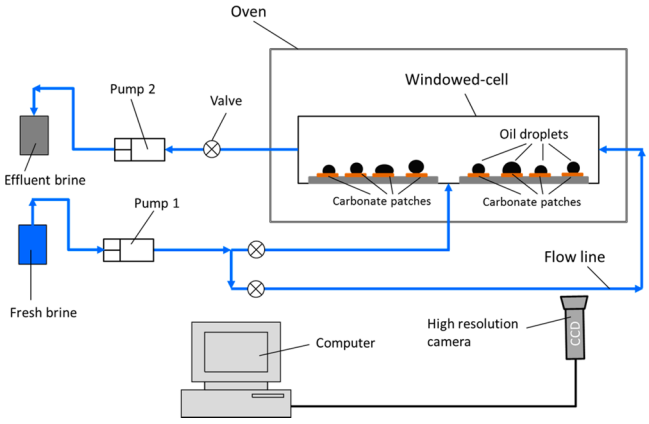

Figure 2. Schematic of the experimental setup.

DOI: 10.1021/ef5023847
Energy Fuels 2015, 29, 1352–1367

Preparation of a Model Carbonate Surface. The mode of preparation of the samples is mostly the same as explained in previous work on clays.[1] Microscope glass slides are used as the base on which artificial carbonate rock surfaces are created. Therefore, they have to be clean and free from any type of contaminants that might prevent total water-wetness. The microscope slides are introduced into an aqueous solution of Hellmanex detergent and undergo an ultrasonic bath for 50−60 min. They are further cleaned with demineralized water and blown dry with nitrogen. After the cleaning step, artificial carbonate rock surfaces (patches) are created on the microscope slides by depositing approximately 3 μL of limestone or dolomite suspensions using a motorized pipet. The suspension concentration was 8000 and 10 000 mg/L for limestone and dolomite, respectively. The used concentration for dolomite was higher because dolomite has a higher grain density than limestone (see Table 2) and settles more rapidly during the transport of suspension from the beaker to the pipet. Following that, the microscope slides are inserted into a desiccator under vacuum for 20−30 min, where the patches become dry and stick to the microscope slides (no glue or epoxy is used). The carbonates obtained by this method are thin (1−10 μm thick), circular-shaped, and have a rough surface. A microscope photograph of the dried patch is presented in Figure 3. The carbonate patches adhere naturally to the microscope glass slides and remain immobile during experiments. Next, small volumes of oil (2−6 μL volume) are attached to the dry carbonate patches while still in contact with air. This procedure is necessary to ensure a direct contact between oil and carbonate and is meant to approximate the initial condition in the reservoir: intermediate or mixed-wet condition.[55−57] In the geological history of an oil reservoir, this condition develops as a consequence of water-film breakage that brings oil directly into contact with the rock surface. This exact mechanism as in actual porous media (i.e., attaching oil on an immersed or a wet carbonate substrate) could not be replicated one-to-one because it requires a high capillary pressure to a thin water film to a level at which film rupture can occur. Because of the lack of capillary pressure, the method of oil attachment to wet surfaces did not lead to a permanent contact. The upside-down approach, where the oil is introduced to surfaces immersed in brine to produce a pendant drop instead of a sessile drop, did not show a permanent attachment. When such a configuration is slightly tilted, the oil droplet will move, indicating that there is no real attachment on the surface, while in our approach, the sessile droplet (after immersion in brine) will remain stationary.

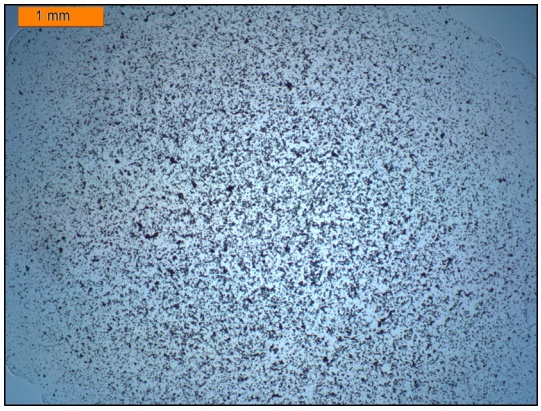

Figure 3. Micro-photograph of a dried carbonate patch.

Finally, the slides with the patches and oil drops are placed inside the cell and are exposed to brines with decreasing salinity in a sequential manner. On each single slide, 7−8 carbonate patches are made to increase the reliability of the measurement results by including the statistical repeatability.

ζ-Potential Measurement. The ζ-potential, which is the potential at the slip plane in the EDL around a charged species, was measured with a Zetasizer Nano-ZS (Malvern Instruments). The instrument measures the electrophoretic mobility of particles in a suspension of carbonate particles or oil droplets dispersed in brine. The ζ-potentials are inferred from the electrophoretic mobility using the Smoluchowski approximation of Henry's equation.

The carbonate suspensions were prepared by mixing 0.2 g of milled carbonate particles below 45 μm with 20 mL of brine, which represents 1% weight of the aqueous solution. For the case of oil, a volume ratio of 1:5 was used by mixing 2 mL of oil with 10 mL of brine. The mixtures were placed in a sweep-enabled sonicator bath for 20 min and allowed to rest for 1 day for equilibration. Whenever a titration was considered, pH was adjusted by manually adding hydrochloric acid (HCl) or sodium hydroxide (NaOH) solution. After the acid or base solution was added, the mixture was stirred for 5 min approximately and allowed to rest for 20 min; meanwhile, the pH was monitored until reaching a constant value.

For carbonate particles, the ζ-potential was measured down to pH 5−6 because, at lower pH values, measurement was not possible as a result of dissolution of carbonate and instability of the measurements. The average value of five measurements with 15−100 runs each was selected as the expected ζ-potential. The error bar was determined on the basis of the standard deviation of the repeated measurements.

Crude/Brine Interfacial Tension (IFT) Measurement. IFT measurements were obtained in a DSA100S, KRUSS GmbH tensiometer. A pendent drop of the oil phase is formed with a special needle in brines with different salinities, and the interfacial tension is measured. A digital image of the pendant drop is acquired and processed, and the shape profile or interfacial contour is determined. The IFT is calculated by fitting the Laplace equation of capillarity to the drop shape profile obtained. The measurements were performed at 25 °C, and the equilibrium values are presented in Table 4. Equilibration was reached after about 500−2000 s. During equilibration, chemical and physical equilibrium is established between oil and the surrounding brine and an IFT decrease was observed. Several measurements were performed for each brine/oil system for reproducibility. All of the repeated measurements yielded similar values.

Table 4. Brine−Oil IFT Measurements

brine	IFT (mN/m) at 25 °C	pH at 25 °C
FW	11.8	6.9
SW	7.2	8.0
25dSW	13.1	7.5
25dSWEQ	8.8	9.2

The IFTs observed fall well into the range of IFT values reported in the literature.[58,59] A potential influence of contamination was ruled out by a detailed FTICR−MS analysis.

Contact Angle Measurement. The acquired high-resolution images of oil on carbonate surfaces were analyzed to determine the contact angle with the substrate. The contact angle was measured according to standard protocols through the denser phase, which is the brine here. The measurement of the contact angle is in the macroscopic region, where the contact angle is not influenced by the surface roughness and there are strong interactions with the solid interface, as sketched in Figure 4. Conventionally, a Young−Laplace (Y−L) fitting to the oil shape profile is applied to determine the contact angle. However, the

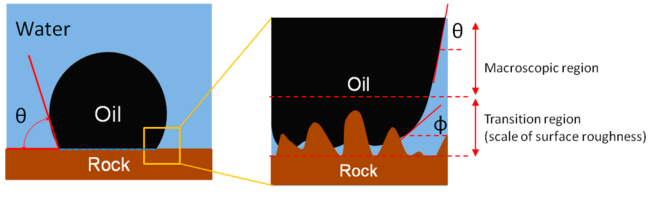

Figure 4. Contact angle measurement: the measurement is in the macroscopic region beyond the reach of carbonate surface roughness and interaction.

DOI: 10.1021/ef5023847
Energy Fuels 2015, 29, 1352−1367

Table 5. Summary of the Conducted Experiments

experiment	step 1	step 2	step 3	step 4
1	FW	SW		
2	FW	25dSW		
3	FW	SW	SW (flow mode)	low-salinity, low-pH NaCl brine (2540 ppm, pH 1.89), flow mode
4	FW	25dSWEQ		

Y−L equation to hold requires smooth solid surfaces with negligible contact angle hysteresis because of pinning. In our case, the Y−L equation could not fit the droplet profile, especially at the contact point with the solid interface because of the surface roughness of the carbonate particles and the distortion of the oil−water interface by the strong contact angle hysteresis. Therefore, the contact angle was determined via matching the oil/brine surface, defining the baseline at the solid interface and determining the tangent to the oil contour. The left and right contact angles of the droplet were both measured, and the arithmetic average was used for further analysis. The measurement error in the contact angle is below ±2° because of the high-resolution images of the droplet.

Experimental Methodology. The fabricated carbonate patches are placed in the windowed cell. The patches are first exposed to FW until the droplet shape reaches a steady state (this typically occurred within 1−2 days) and then are exposed to lower salinity brines. Brine exchange in the cell is performed by flowing brine to the cell with pump 1 and removing the existing brine (e.g., FW) from the cell with pump 2. This continues until the cell is completely filled with new brine at which point the conductivity of the effluent brine corresponds to the conductivity of injection brine. In each step of salinity, the shape of the oil droplets is continuously monitored by the digital camera. The experiments with FW and low salinity continue until no further change in contact angle is observed. Because there is no viscous flow or flow-driven lift force in the cell (except at the beginning of the experiment when brines are exchanged), oil shape and release are solely driven by the balance of buoyancy and adhesion forces. Because the buoyancy force can be assumed constant during each of the high- and low-salinity phases because of constant oil volume and approximately constant density, oil detachment merely reflects the reduction in oil adhesion to the carbonate.

Experiments were designed such that we can investigate different wettability alteration mechanisms, such as calcite dissolution and surface charge change. In our approach, we designed experiments in such a way that the surface charge change mechanism can be investigated by first eliminating the dissolution effect, whereas in another type of experiment, the dissolution is enhanced and surface charge effect is suppressed. A summary of the experiments is given in Table 5. All of experiments are conducted at a constant temperature (25 °C). During each experiment, the pH of the brine in the cell before and after each step is recorded.

RESULTS

ζ-Potential for Limestone and Dolomite as a Function of Salinity and pH. Below, we will examine the ζ-potential of the limestone and dolomite rocks used in our oil droplet experiments.

Limestone Particles. The ζ-potential of limestone particles in various brines is shown in Figure 5. At first glance, a clear trend stands out: at all salinities, the ζ-potential increases when the pH increases. This implies that, at higher pH, the surface charge of limestone becomes more positive.

In FW, the surface charges of limestone particles remain positive (from +5.2 to +7.4 mV) over the pH range covered, while the ζ-potential values increase slightly with pH. In SW, the change of ζ-potential with pH is more pronounced, with a negative value around −6 mV at pH 6.6 up to the isoelectric point (IEP) at pH 9.4. Beyond the IEP, the ζ-potential is positive, +3.75 mV at pH 10. SW has both lower salinity than

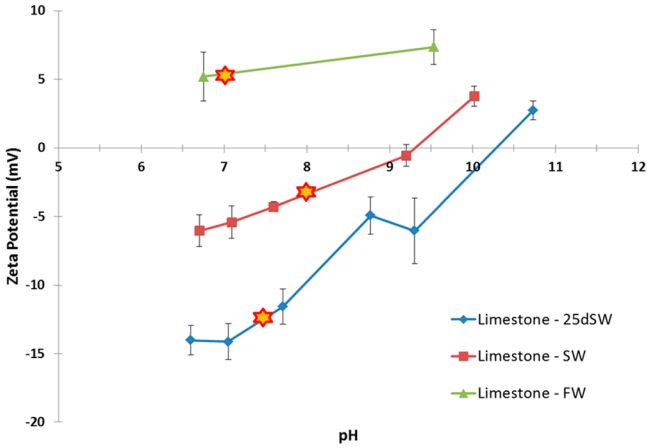

Figure 5. ζ-potential of limestone particles in FW, SW, and 25dSW throughout the pH range of 6.5−11 (yellow stars represent the natural pH of the brines).

FW and higher SO_4^{2-} concentration, which together result in less positive ζ-potential with SW than with FW over the pH range covered. The ζ-potential values of the limestone particles in 25dSW are much more negative and significantly sensitive to pH because the slope of the curve is higher than that of FW and SW. The IEP is at pH 10.3. Clearly, the IEP does vary with brine salinity.

The extent to which pH change causes a small or large shift of ζ-potential seems to depend upon salinity. Indeed, the higher the brine salinity, the smaller the gradient of ζ-potential with pH. We believe that this effect occurs because, in high-salinity brine, such as FW, the binding sites at the surface of particles are overcrowded with potential-determining ions, as is the EDL, and these ions compete for surface sites. Because the concentration of Ca^{2+}, Mg^{2+}, and SO_4^{2-} is substantially greater than the concentration of H^+ and OH^-, any change in the concentration of the former ions would be strongly felt inside the EDL and affect the ζ-potential considerably. Therefore, at high-salinity conditions, any change in the concentration of H^+ or OH^- (change in pH) would not have a significant effect on ζ-potential because H^+ can react with SO_4^{2-} and Ca^{2+} and Mg^{2+} can react with OH^-. This would require them to penetrate a compressed and shrunk EDL though to influence the ζ-potential.

Dolomite Particles. For dolomite particles, in all of the brines, the IEPs are shifted 2−3 pH units toward the left, indicating that the surface charges are more positive than those of limestone particles, as Figure 6 indicates. The particles in FW and SW have positive surface charges throughout the studied pH range. Moreover, a pH change has a minimal effect on the ζ-potential values in the brines mentioned above, unlike for 25dSW, where the ζ-potential is strongly sensitive to pH change. The respective IEP is 8.2.

This is already an indication that dolomite particles react differently in comparison to limestone particles and exhibit

DOI: 10.1021/ef5023847
Energy Fuels 2015, 29, 1352−1367

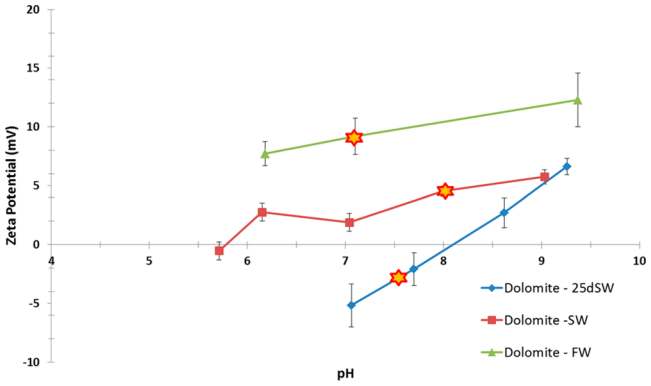

Figure 6. ζ-potential of Silurian dolomite particles in FW, SW, and 25dSW throughout the pH range of 5.5−11 (yellow stars represent the natural pH of brine).

more positive surface charges as inferred from ζ-potential for dolomite versus limestone. For comparison, the ζ-potential of limestone and dolomite at pH 7.0 and different brine salinities is shown in Figure 7. Explanation of this observation is rather

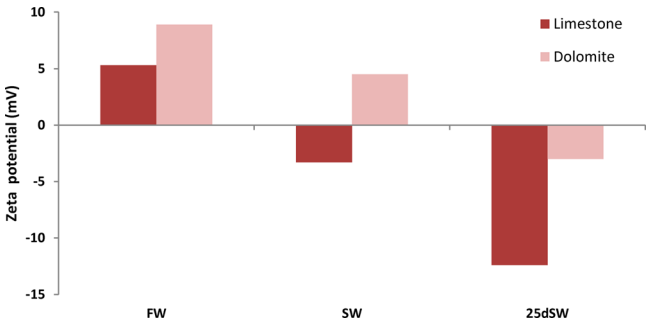

Figure 7. ζ-potential of limestone and dolomite particles in FW, SW, and 25dSW at pH 7.0.

complex and requires looking at the surface speciation reactions, which could provide clues on why calcite and dolomite behave differently.

From a mineralogy perspective, this could be attributed to the additional presence of magnesium in the crystalline lattice when compared to calcium carbonate minerals, which lack magnesium. The surface species that are exposed at calcite or dolomite are $>Me^+$ and $>CO_3^-$ (Me = Ca and Mg). The surface density of these sites, which are the basis for sorption of PDIs from brine (H^+, OH^-, CO_3^{2-}, Ca^{2+}, and Mg^{2+}), was reported to be 5 and 8 sites/nm^2 for calcite and dolomite, respectively.[49] A higher number of sorption sites for dolomite versus calcite could potentially allow for higher positive charges at the dolomite/brine interface.

From an EDL perspective, a study performed by Mielczarski et al.[51] shows that the EDL capacitance (or the amount of electric charge or energy stored by means of the double-layer effect) for dolomite is larger than that for calcite (15 F/m^2 for calcite and 25 F/m^2 for dolomite at an ionic strength of 0.01 M NaCl). Their conclusion is that the EDL is thin, highly structured, and non-diffuse and, therefore, can accommodate high charge densities. The high surface charge density is such that the brine ionic strength has only a small influence on it.[49] The higher EDL capacitance for dolomite allows for the buildup of a higher surface charge density than that for calcite.

Effect of Mineral Precipitation on ζ-Potential. In principle, only one equilibrium point between brine and carbonate minerals exist, which has a specific pH. When the pH is changed, this equilibrium changes, which can result in precipitation. There are several ways to approach this. One is to adjust pH before equilibration with carbonate particles; however, the brine composition changes upon contact with minerals, and one would obtain a different pH. One can equilibrate before pH change, and then there is the risk of precipitation. In our study, we chose this approach.

In this section, we explain why the upward trend of the ζ-potential with pH is real. A more detailed explanation of the trends, involving surface complexation modeling, will be presented in a future publication.

In the ζ-potential measurements, the solution pH was adjusted using either acid or base solution. At increased pH or alkalinity precipitation of Ca^{2+} and Mg^{2+} from the solution is expected; however, this phenomenon could not have changed the trends significantly. This can be confirmed by a number of compelling reasons and evidence: (i) the conductivity of the solution was monitored during the measurements, which suggests that there was no change of ionic strength. Actually, change of the ionic strength because of precipitation is minor (within 1%), as confirmed by PHREEQC simulations. (ii) There was no visual sign of precipitation. (iii) The formation of surface charge happens faster than the precipitation. The ζ-potential measurements were made approximately 20 min after changing the pH. Precipitation, as confirmed by laboratory tests, is a slow process and requires longer times, particularly, at lower salinities and low alkalinity. (iv) Another piece of evidence is the results in 25dSW. On the basis of the PHREEQC simulations, the saturation pH is about 9.3 at 25 °C. This means that, only at pH exceeding 9.3, mineral precipitation can occur. As the data in Figures 5 and 6 show, most of the measurements are in the range of 6.5 < pH < 9.2, where precipitation was unlikely to happen. Moreover, at pH beyond 9.3, there is no sign of sharp change in the ζ-potential, which could be triggered by precipitation. For SW, the saturation pH is about 7.3, which is lower than that of 25dSW because of the higher calcium concentration and alkalinity (as HCO_3^-). For SW beyond pH 7.3, precipitation could occur, but again, no sharp change in the ζ-potential was observed. A further check was performed using SW brine without carbonate particles (a blank test). Several samples were prepared where pH was increased from 8.0 to 11.0 by adding NaOH solution. Even after a few hours, precipitation (which was likely) was below the detection limit or minor and the solutions were clear. Only at pH > 10, precipitate started increasing and the samples appeared milky. We attempted measurement of ζ-potential with all samples. For samples with pH < 9, the measurements were not stable and unreliable because of the fact that the concentration of particles was too small or the particles were non-existent. For the rest of the samples, the measured ζ-potential showed that the precipitate is negatively charged (average value = −3.4 mV at pH 10) and the ζ-potential varied slightly with pH. These measurements imply that, first, precipitation below pH < 10 is insignificant compared to pH > 10. Because most of the actual data in Figures 5 and 6 are at pH < 10, therefore, the effect of precipitation on the data is negligible. Second, the ζ-potential of the precipitate is quite different from that of limestone and dolomite particles.

Hence, from above, we can conclude that the upward trend of ζ-potential with pH has been developed by the interactions

DOI: 10.1021/ef5023847
Energy Fuels 2015, 29, 1352−1367

(complexation reactions) between the PDIs in the solution and the surface species at the carbonate surface and are the result of using brine compositions naturally occurring in the carbonate formations. Alotaibi et al.[53] has observed a similar trend, as discussed earlier.

ζ-Potential for Oil as a Function of Salinity and pH. The ζ-potential measurements of oil emulsion in FW, SW, and 25dSW are shown in Figure 8. As generally expected (because

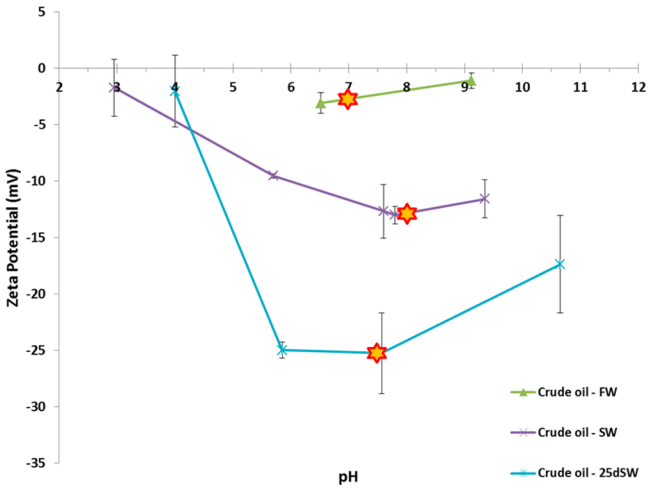

Figure 8. ζ-potential of oil droplets in FW, SW, and 25dSW brines (the yellow stars represent the natural pH of the brines).

of the presence of carboxylic acid groups and phenols with low pK_a in the oil), the surface charges at the oil/brine interface are negative and decrease even further with decreasing brine salinity. Oil particles in FW have a slightly negative ζ-potential, albeit close to zero. Only a few points could be measured for FW because, at higher pH, the measurements did not stabilize. The ζ-potential values in SW are more negative (around −12 mV) and decrease further in 25dSW (from −25 to −17 mV for 6 < pH < 10.5). For the case of SW and 25dSW, by lowering pH below 7.0, the ζ-potential tends to become less negative and, by further reduction of pH to around 3−4, the negative charges at the oil−brine interface are neutralized and ζ-potential reaches close to zero values (IEP).

Overall, the measurements at higher pH (exceeding 9−10) were not as stable. With respect to the earlier discussion, the ζ-potential (including the upturn at pH ≈ 8 in SW and 25dSW) is unlikely to be affected by the mineral precipitation, thus dominated by the chemical interactions at the oil/brine interface between the ions in the brine and the polar functional groups (acidic and basic species) in the oil.

Wettability Alteration (Contact Angle Change) as a Function of Brine Composition. In this section, first, we demonstrate the LSE in SW. Then the results using 25dSW are presented where dissolution is possible. In the next experiment, mineral dissolution is enhanced using low-salinity brine at low pH and the associated effect on rock wettability is investigated. In the last experiment, the results with 25dSWEQ are presented to examine the LSE in the absence of mineral dissolution and the role of double-layer electrostatic force in wettability alteration.

Please note that the initial contact angles in individual experiments, even on the same type of carbonate rock, can vary significantly. The contact angle observed here is a macroscopic, effective contact angle, which is subject to contact angle hysteresis and influence by roughness and other factors, including the preparation procedure. Except for very ideal and atomically smooth surfaces, macroscopic contact angles are different from the intrinsic contact angle,[60] but using such ideal surfaces is not following the fundamental philosophy of our study. We should emphasize that what is more important is the actual trend of the contact angle change after exposure to low-salinity brine rather than the initial value of the contact angle.

Demonstration of the LSF Effect with SW. The carbonate patches used in this experiment are limestone and dolomite patches on which oil droplets are deposited. The samples reside altogether inside the windowed cell and remain exposed to FW until a stable contact angle (i.e., an equilibrium state) is reached. The FW is replaced by SW as low-salinity brine. For clarity, a subset of the representative results is presented in Figure 9. The results show that, in FW, the shape of oil drops tends to reach an equilibrium state, after which their contact angle remains constant. When switching over to SW after 40 h, the contact angles for both oil droplets on limestone as well as dolomite decrease by ca. 5−17°. This is illustrated in Figure 10.

Table 6 shows the pH of the brines at the start and end of their residence time in the windowed cell. As seen, the pH in this experiment did not change significantly and the small change observed is within the margin of the measurement error. This is in agreement with PHREEQC calculations and ICP−

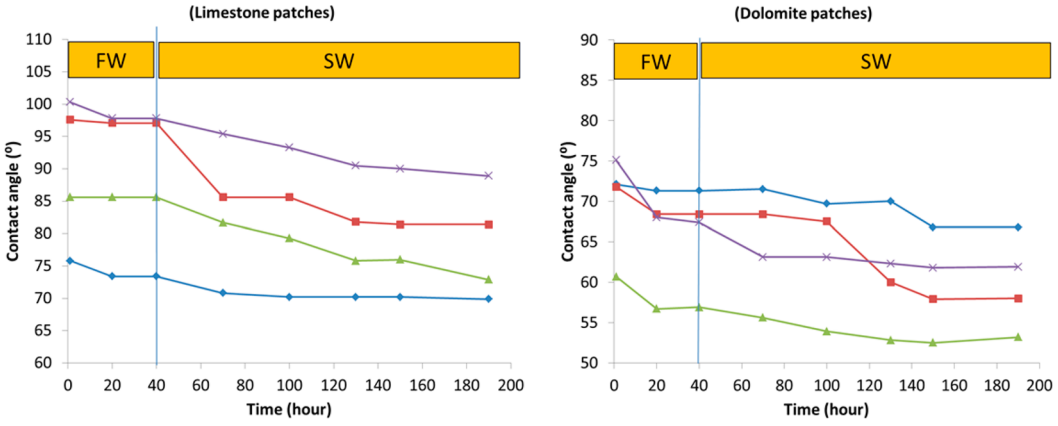

Figure 9. Contact angle of four different oil droplets (with different curve colors) on (left) limestone and (right) dolomite patches as a function of time in FW and SW.

DOI: 10.1021/ef5023847
Energy Fuels 2015, 29, 1352−1367

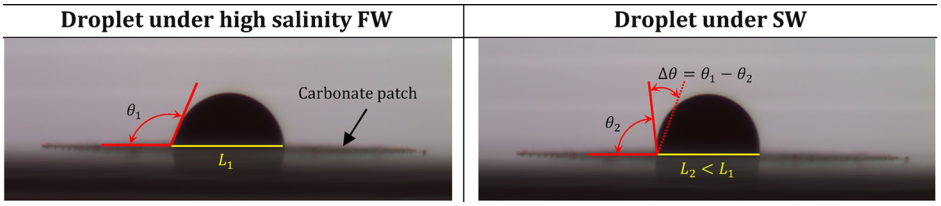

Figure 10. Oil droplet contact angle on limestone under high-salinity FW and SW. L denotes the diameter of the oil−carbonate contact line, which decreases along with the contact angle.

Table 6. pH of FW and SW Brines at the Start and End of Their Residence Time in the Cell

brine	pH_{start}	pH_{end}
FW	6.9	6.9
SW	8.0	8.0

Table 7. pH of FW and 25dSW Brines at the Start and End of Their Residence Time in the Cell

brine	pH_{start}	pH_{end}
FW	6.9	6.9
25dSW	7.5	8.7

MS measurements (see Appendix 2 of the Supporting Information), confirming that no dissolution is occurring in SW. There is precipitation/sorption of Ca^{2+} and Mg^{2+} though.

Results in the Presence of Mineral Dissolution with 25dSW. As before, limestone and dolomite patches were used in this experiment. As confirmed by a PHREEQC model and solubility data from ICP−MS (in Appendix 2 of the Supporting Information), 25dSW brine has the ability to dissolve limestone and to a lesser extent dolomite. The carbonate solubility is about 9 ppm (as obtained from ICP−MS) and about 3 ppm from PHREEQC simulations. This shows that the brine salinity increase as a result of calcite dissolution is in the order of 10 ppm, which is insignificant compared to the total brine salinity. However, calcite dissolution increases pH by 1.2 units, which has a larger impact on the surface charges than the salinity change alone.

The contact angle results presented in Figure 11 show that, in FW, the contact angle of oil droplets reaches a constant value after attaining the equilibrium state, just as in the results previously discussed. When switching over to 25dSW, a decrease in the contact angle is only observed for oil droplets on limestone. Exposure of oil droplets to 25dSW lasted for approximately 100 h, and the decrease in the contact angle is in the order of 5−17°.

Table 7 shows the pH of the brines during the experiment. An increase in pH of 25dSW clearly indicates that limestone dissolution has occurred. Furthermore, calcium carbonate mineral or calcite has higher solubility than dolomite. It is expected that dissolution of limestone, which is mainly composed of calcite, would have occurred faster and triggered pH change. This could prevent the dissolution of dolomite particles.

Although the same results are obtained when the experiments are repeated, there was one experiment in which 25dSW caused contact angle change for oil drops on dolomite patches. In that experiment the starting contact angles were small (~40°). In this case, oil detachment was observed.

Enhanced Dissolution by Low-Salinity NaCl Brine at Low pH. This experiment was performed to understand the effect of rock dissolution on the wettability change of the carbonate patches. The patches used in this experiment consisted of dolomite. First, the system was exposed to FW and SW under static conditions. All oil droplets experienced some contact angle decrease in the range of 5−15° in SW after 150 h (Figure 12). Subsequently, SW was injected at a flow rate of 7.5 mL/min for 2 h. This flow rate is the maximum that the pumps could handle. Note that there was no noticeable disturbance of any oil droplet by the flow of the brine. In the last step, NaCl brine (2540 ppm) at pH 1.89 was injected into the cell for approximately 2 h under the same flow conditions. A sharp decrease of the contact angle (5−15°) for all oil droplets was the result, which continued over the entire period of 2 h.

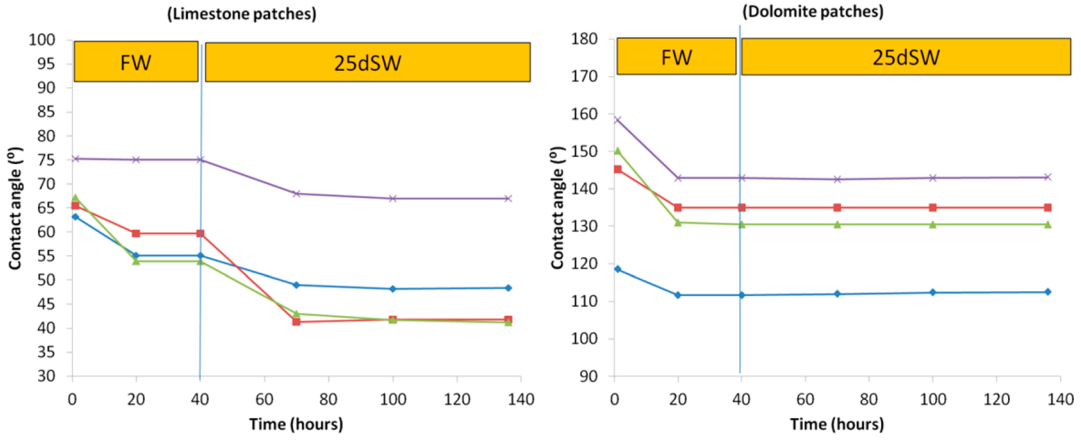

Figure 11. Contact angle of four oil droplets (with different curve colors) on (left) limestone and (right) dolomite patches as a function of time in FW and 25dSW.

DOI: 10.1021/ef5023847
Energy Fuels 2015, 29, 1352−1367

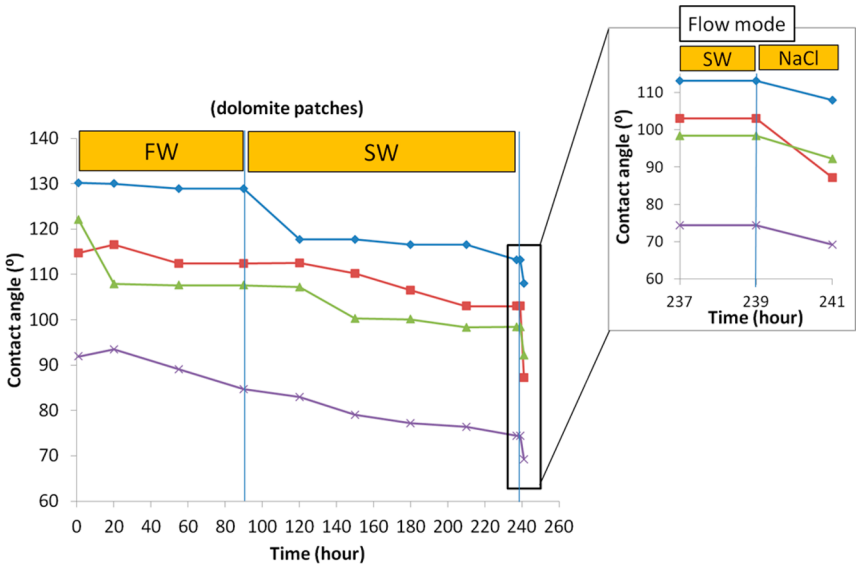

Figure 12. Contact angle of oil droplets on dolomite patches as a function of time in FW, SW, and low-salinity NaCl brine at pH 1.89.

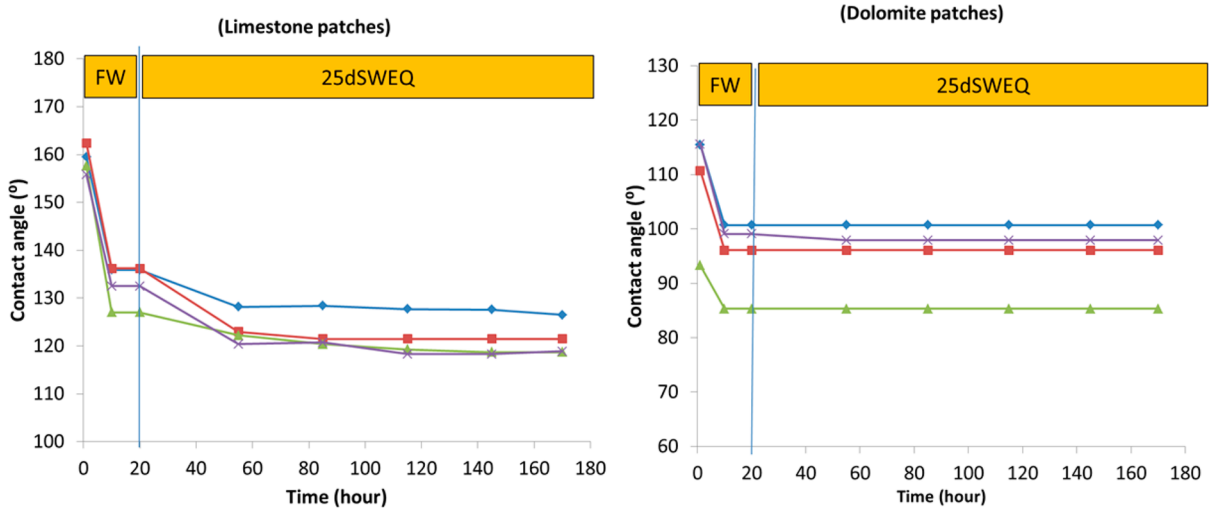

Figure 13. Contact angle of four oil droplets (with different curve colors) on (left) limestone and (right) dolomite patches as a function of time in FW and 25dSWEQ.

Because of flow, the pH change of the brine was very small. Because, at low pH, dolomite dissolution is fast, the recession of the three-phase contact line could have been caused predominantly by dolomite dissolution at the three-phase contact point. The flow of brine can be excluded as a reason because, in the SW, the flow experiment described above did not cause any contact angle change.

Results in the Absence of Mineral Dissolution with 25dSWEQ. Likewise, limestone and dolomite patches onto which oil drops were deposited were used in this experiment. 25dSW has been equilibrated with limestone for 1 week prior to starting the experiment, to ensure that the brine becomes saturated with calcium, so that no mineral dissolution occurs in the cell. Figure 13 shows some of the results obtained from the experiment. The oil droplets on limestone and dolomite patches resided in FW brine initially until equilibrium was reached after 20 h. A contact angle change in the range of 5−10° is observed only for oil droplets on limestone. The oil droplets on dolomite did not experience any change in the contact angle nor shape throughout their exposure to 25dSWEQ brine.

Table 8 shows the pH of the brines at the start and end of their residence time in the cell. Again, no pH change is recorded because the brines do not induce any limestone or dolomite dissolution.

Table 8. pH of FW and 25dSWEQ Brines at the Start and End of Their Residence Time in the Cell

brine	pH_{start}	pH_{end}
FW	6.9	6.9
25dSWEQ	9.2	9.2

DISCUSSION

The model system experiments were designed to demonstrate the LSE when brine salinity or composition is lowered or altered and to scrutinize the two likely key mechanisms of wettability alteration by low-salinity brine: (i) mineral

DOI: 10.1021/ef5023847
Energy Fuels 2015, 29, 1352−1367

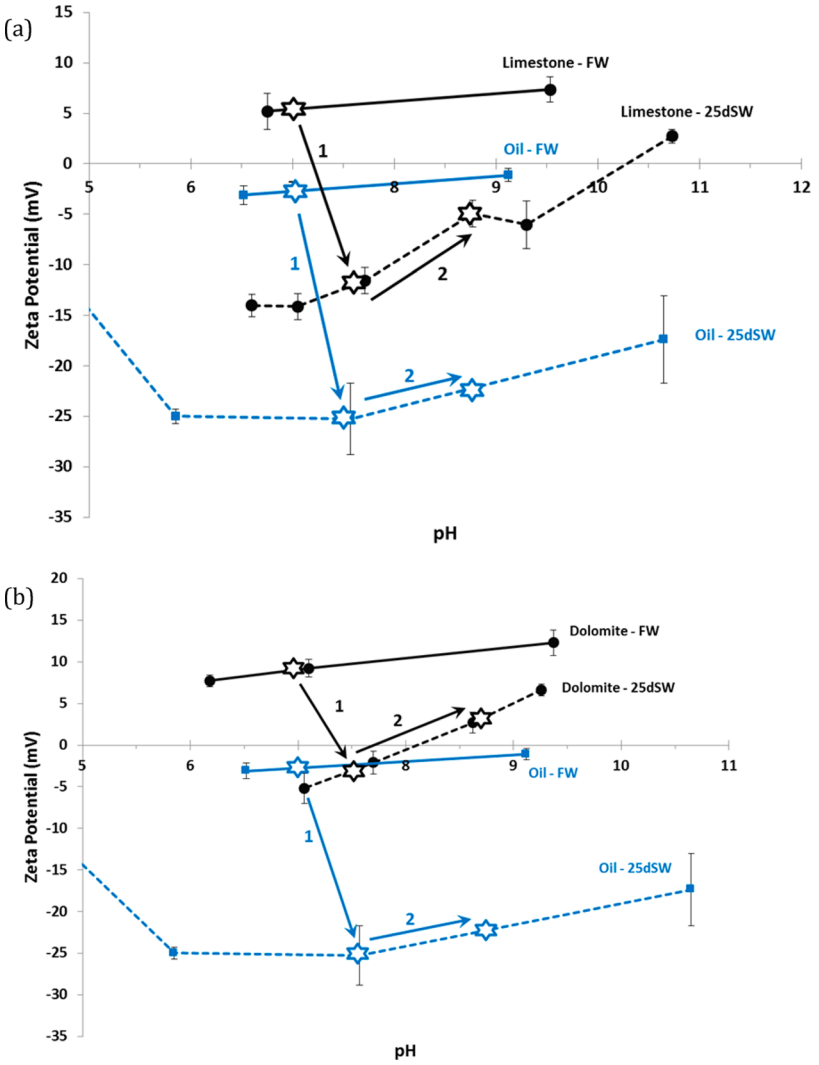

Figure 14. Change of oil and rock ζ-potential upon reduction of salinity from FW to 25dSW: (a) results for limestone and (b) results for dolomite. In each panel, step 1 designates change of ζ-potential for rock or oil upon change of salinity and step 2 designates ζ-potential change caused by the pH increase of the brine because of mineral dissolution. The stars represent the pH of the brines.

dissolution and (ii) surface charge change (electrostatic repulsion between carbonate/brine and brine/oil interfaces).

In the experiment with 25dSW brine, both dissolution and surface charge change can take place; therefore, the two effects cannot be completely separated. Interestingly, this low-salinity brine triggered a contact angle decrease for oil drops attached to limestone patches, whereas the contact angle of oil drops on dolomite patches remained constant. Here, 25dSW has supposedly dissolved part of the limestone/dolomite patches, causing an increase in pH. Furthermore, the analysis of ICP–MS data has shown that dolomite dissolves much less compared to limestone in 25dSW. Therefore, limestone patches experienced much more dissolution than the dolomite patches.

Consistent with the data on the contact angle change for oil droplets on the patches, the ζ-potential of limestone particles in 25dSW at pH 7.5 is negative (−13 mV) and, as pH increases with limestone dissolution, ζ-potential reaches −6 mV. In addition, the more negative surface charges created at the oil surface cause enough electrostatic repulsion to change the wettability of the rock, which translates into a decrease of the contact angle. Dolomite particles on the other hand exhibit a positive ζ-potential (+3.0 mV) in 25dSW at pH 8.7 (equilibrium pH), although lower than their ζ-potential in FW brine (+9 mV). However, in 25dSW, the ζ-potential difference (gap) between oil and dolomite substantially increases, which could explain why no contact angle change (or wettability alteration) was observed for oil droplets on dolomite. This is illustrated in Figure 14, which combines the data from oil–brine and mineral–brine surfaces.

In the other experiments with SW and 25dSWEQ, mineral dissolution was eliminated, which allows for investigation of the influence of surface charge change on rock wettability alteration by low-salinity brine. As illustrated in Figure 9, SW caused a contact angle decrease for all oil drops in the absence of any carbonate dissolution. Likewise, 25dSWEQ brine triggered a contact angle decrease, although only for oil droplets bound to limestone patches.

In the experiments where SW is used, an analysis of the ζ-potential data shows that FW with pH 6.9 causes positive charges at the surface of both limestone and dolomite particles, +5.3 and +9 mV, respectively. SW, in contrast, at pH 8.0 induces lower ζ-potential for limestone and dolomite, −4 and +4 mV, respectively. In addition, the surface charges at the oil/brine interface are more negative (Figure 8). The more negative

DOI: 10.1021/ef5023847
Energy Fuels 2015, 29, 1352–1367

surface charge could cause a stronger repulsion at the oil−brine−rock contact, forcing the three-phase contact line. The process happens progressively, and while the contact line recedes, the contact angle decreases gradually. For dolomite patches in SW, the force between oil and dolomite remains attractive; however, it is the magnitude that should have decreased and, thus, resulted in recession of the contact line under the act of buoyancy force. SW has a considerably larger SO_4^{2-} concentration than FW (~14 times), and according to the previous studies reviewed in the Introduction, SO_4^{2-} can adsorb preferentially at the three-phase contact line; therefore, rock ζ-potential is reduced, and because of its (SO_4^{2-}) size, it increases the separation distance between oil and dolomite. A combination of ζ-potential decrease (less positive) and increase of the separation distance can sufficiently reduce the electrostatic adhesion force between oil and dolomite.

In the experiment where 25dSWEQ with pH 9.2 was used as low-salinity brine, ζ-potential data show negative ζ-potential (−6 mV) on limestone particles and positive ζ-potential (+6.6 mV) on dolomite particles, which is slightly lower than those in FW. This implies that, by switching from FW over to 25dSWEQ, the electric charges on limestone patches become negative, while they remain as positive at the dolomite surface. In addition, the charges at the oil surface are in both cases more negative. As a result, there is certainly more repulsion at the limestone patches and more attraction at the dolomite patches. This could be the reason why there is a contact angle change only for oil drops on limestone patches.

A comparison of the results for limestone and dolomite patches indicates that the mechanism responsible for the observed wettability change of the rock in the systems studied by us is caused by changes at the rock/brine interface and at least less by changes at the oil−water interface. If we consider the IFT data, we notice that SW has 3−4 units lower IFT than FW. One could therefore argue that a decrease in IFT could have driven the decrease in the contact angle. However, 25dSWEQ brine has a lower IFT than FW, as is the case with SW. Only oil droplets located on the limestone patches showed a contact angle change when 25dSWEQ replaced FW. The fact that oil drops on dolomite patches behave differently implies that the IFT change alone is not responsible for the decrease of the contact angle of the oil drops; otherwise, irrespective of the type of patch, oil drops are expected to behave similarly at least. Furthermore, 25dSW brine has a higher IFT than FW; still, a contact angle decrease was observed. Moreover, oil droplets are strongly bound to the carbonate patches by forming pinning points. Consequently, the three-phase contact line can only move if these bonds at the pinning points are weakened or broken. This appears unlikely to happen with a small change in IFT only.

A change in the contact angle for oil drops on dolomite was observed only when the starting values at the point of injection of low-salinity brine were around 40°, which implies already quite weak adhesion forces between oil drops and dolomite patches. In such a case, even a small change in electrostatic forces because of a decrease in surface charges should be enough to trigger a contact angle decrease. On the other hand, when the starting contact angles were much higher, no contact angle change was observed for oil drops on dolomite. A similar relationship has been observed by Mahani et al.[1] between the initial contact angle and volume of droplet over its contact area with the solid (V/A) for the case of the detachment time of oil droplets from clays. This detachment time was found larger for droplets with an initially large contact angle than for those with a smaller contact angle. An explanation could be that more spreading oil droplets have a larger contact area with the solid surface and, given the roughness of the carbonate surface, the actual contact area is larger than the apparent (macroscopic) contact area of the droplet with the surface, therefore resulting in a larger adhesion force or smaller detachment (buoyancy) over adhesion force at the contact line.

It appears that the above observation holds over a wide range of initial contact angles, where a smaller response (i.e., contact angle change) to a change of salinity is observed for dolomite than for limestone. This is shown in Figure 15. This suggests

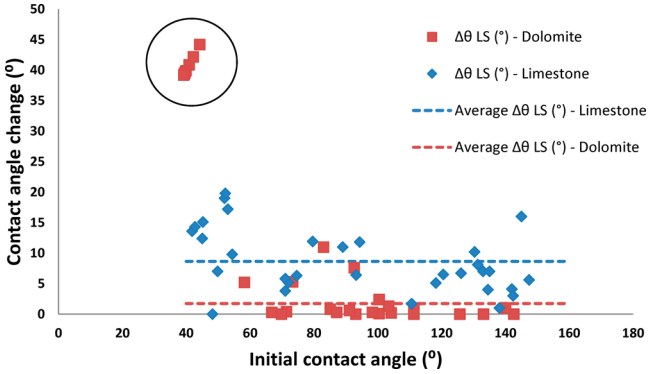

Figure 15. Contact angle change for oil on limestone and dolomite in SW, 25dSW, and 25dSWEQ brines versus the initial contact angle at the start of low-salinity exposure. The circled data denote the results with dolomite patches, where the initial contact angle at the start of low salinity was about 40°. Only in this case, a large LSE (or contact angle change) was observed, leading to detachment of oil from the dolomite patches.

that oil detachment from a dolomite surface requires larger forces at the contact line because the adhesion between dolomite and oil is stronger than for limestone.

To shed some more light on the differences in response to low-salinity brine between limestone and dolomite surfaces, a look at the disjoining pressure at the carbonate/water and oil/water interfaces appears worthwhile. The disjoining pressure comprises of electrostatic, van der Waals, and structural components. The electrostatic component, which results from the EDL forces between two surfaces with different potentials, is a long-range force and, for strongly charged systems, often the dominant factor. To estimate the force between oil and carbonate, we focus on the electrostatic component of the disjoining pressure, as suggested by the ζ-potential behavior illustrated by Figures 5−8, pointing at electrostatic interactions playing a dominant role. The geometry of oil and rock surfaces is simplified as flat-charged surfaces with different potentials, separated by a thin film of electrolyte. McCormak et al.[61] presented a general equation for the electrostatic force between two parallel charged surfaces, which can be adapted for our system comprising oil and carbonate surfaces. For this system, the electrostatic forces per unit area (or pressure) acting between the surfaces is given by the sum of an osmotic term and Maxwell stress. At small separations, the Maxwell stress term dominates, which yields

$$\frac{\text{force}}{\text{area}} = P \rightarrow -\frac{\varepsilon}{8\pi}\left(\frac{\zeta_O - \zeta_R}{d}\right)^2, \quad d \rightarrow 0$$

DOI: 10.1021/ef5023847
Energy Fuels 2015, 29, 1352−1367

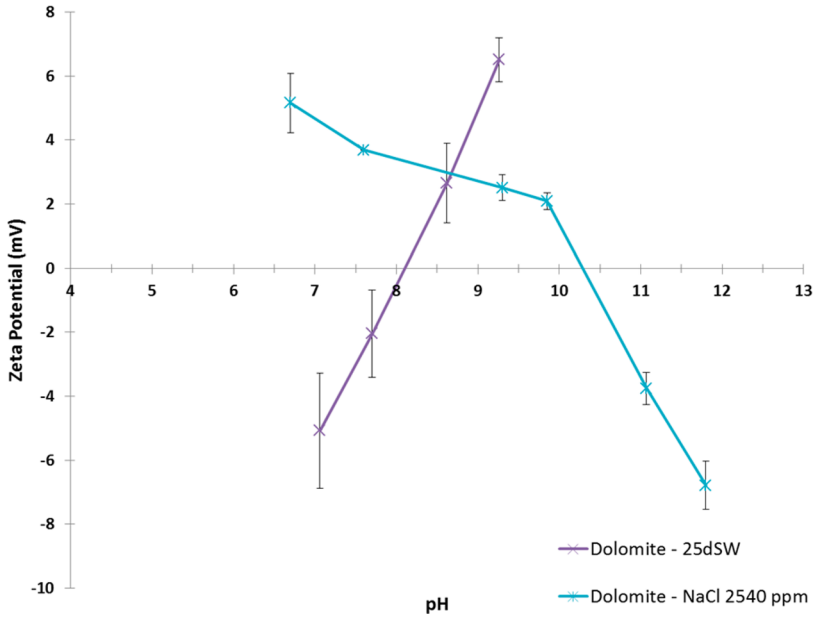

Figure 16. ζ-potential of dolomite in 2540 ppm of NaCl and in 25dSW throughout the pH range of 6.7−12.

where ζ_O and ζ_R are the ζ-potential for oil and rock, respectively, d denotes the film thickness, and ϵ denotes the permittivity of the brine. This equation is valid for potentials of the same or opposite sign at small separations.

From this derivation, it is noted that the magnitude of the force per unit area is proportional to the potential difference between rock and oil = $(\zeta_O - \zeta_R)^2$. On the basis of the different signs of the potentials between oil and carbonate in high-salinity FW (see Figure 14), the electrostatic force is then attractive, which is expected, given the oil-wet nature of carbonate rock. Using this approximation, we can estimate the ratio of adhesion forces for the situation of dolomite versus limestone, assuming equal film or separation thickness.

$$\left.\frac{F_{(\text{oil}-\text{dolomite})}}{F_{(\text{oil}-\text{limestone})}}\right|_{\text{FW}} = \left.\left(\frac{\zeta_O - \zeta_{\text{dolomite}}}{\zeta_O - \zeta_{\text{limestone}}}\right)^2\right|_{\text{FW}}$$

$$= \left(\frac{-2.5 - 9.0}{-2.5 - 5.3}\right)^2 = 2.2$$

Thus, it is clear that, in FW, oil is more strongly bound to dolomite particles than limestone. Moreover, according to Figure 7, the change of ζ-potential with salinity is smaller for dolomite than limestone. Both larger adhesion force and smaller change of ζ-potential with salinity are underlying the smaller LSE with dolomite than limestone. This means that, for dolomite, wettability alteration (contact line recession and/or, subsequently, oil detachment) demands larger reduction of adhesion force at the rock−oil−brine interface. This requires further manipulation of brine composition.

Effect of Mineral Dissolution on Wettability Alteration. The effect of mineral dissolution is well-observed when low-salinity NaCl brine at pH 1.89 is injected in the cell. Prior to that, we see that the flow of SW for 2 h did not cause a contact angle change, because SW is not able to dissolve calcite or dolomite. In addition, the normal time scale of the contact angle change observed during our experiments is rather large. Therefore, we did not expect an observable contact angle decrease during the 2 h period of SW flow. When switching to acidic NaCl brine, the contact angle of all of the oil drops started decreasing sharply, indicating a strong wettability change. This is due to the fact that, at such a low pH, the diffusion of H^+ ions is enhanced by not only the flow of the brine but also their high concentration. Dissolution in this case is transport-controlled or, in other words, dependent upon mass transfer. The aggressive dissolution of the dolomite patches caused the three-phase contact line to recede fast enough that the contact angle value fell in the 2 h period. According to Compton and Daly[62] and Wallin and Bjerle,[63] at the surface of particles, H^+ ions diffuse and protonate the carbonate sites, forcing the release of calcium and magnesium. The release of these ions breaks the bond at the pinning point. When this occurs, there is a sudden jump of the oil tail from the broken pinning point to the next adjacent pinning point.

To understand the relative contributions of the change in surface charge to this contact angle change, we measured the ζ-potential for dolomite in pure NaCl brine as well as other brines (refer to Figure 16). It is noted that the NaCl brine exhibits a reverse trend with pH compared to SW and 25dSW (which contain Ca^{2+}, Mg^{2+}, and SO_4^{2-} in addition to Na^+). For NaCl brine, a decrease of pH reduces the negative charge of the brine/rock interface via protonation of carbonate to bicarbonate ions. A similar behavior was reported by Van Cappellen et al.[49] and Kim and Kovscek.[64] At low pH values (around 2), the charge at the interface is reduced as is the oil−rock repulsion. As such, we expect that, using NaCl brine (at low pH) instead of SW or 25dSW at the same pH, the contribution of electrostatic repulsion is considerably reduced. Consequently, dissolution is more likely responsible for the sharp decrease of the contact angle observed in Figure 12. However, this observation is not relevant to LSF because, in practice, the low-salinity brines have mostly pH greater than 5 and, if carbonate dissolution occurs, it would not be significant, as shown by PHREEQC simulations. A continuous dissolution of a considerable amount of carbonate is required to recede the contact line, requiring the injection of large amounts of acid.

One may wonder whether the LSF effect can be enhanced by making dissolution and electrostatic repulsion work together.

DOI: 10.1021/ef5023847
Energy Fuels 2015, 29, 1352−1367

From the data presented for SW, 25dSW, and 25dSWEQ brines (see Figure 17), it could not be clearly concluded that

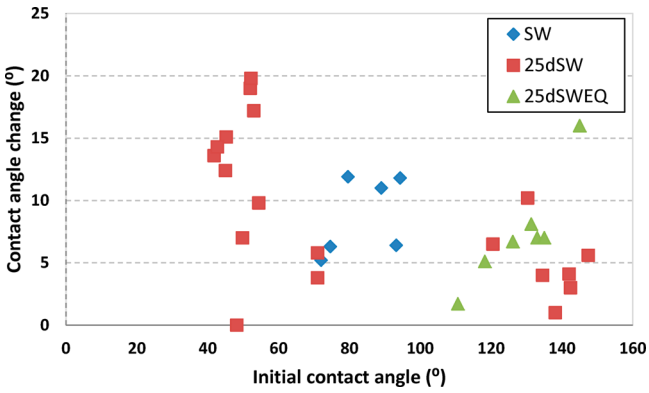

Figure 17. Contact angle change for oil on limestone in SW, 25dSW, and 25dSWEQ versus the initial contact angle at the beginning of low salinity.

dissolution (in 25dSW) enhanced wettability alteration or increased contact angle change. The reason is that samples could not be reproducibly prepared in all experiments. Variations in grain density between patches are difficult to prevent. The initial contact angles also varied between patches, which reduces the precision of contact angle change determination. This precludes a direct comparison. However, from the experiment performed with low-salinity NaCl brine at low pH, it is expected that dissolution enhances the wettability alteration. Nonetheless, mineral dissolution as a mechanism is only relevant in the laboratory. In field operations, the brine will obviously very quickly equilibrate with the carbonates. The concomitant neutralization of the acid would stop dissolution, leaving no contribution to LSE.

Nonetheless, as a result of slight calcite or dolomite dissolution, the pH increases. This pH increase, in turn, could superimpose positive and negative contributions to the LSE. On the one hand, it may suppress wettability alteration because surface charges at the carbonate−brine interface become more positive at higher pH (except for NaCl brine, where an opposite ζ-potential−pH trend is observed). On the other hand, a pH increase may also reduce the brine/oil IFT because of saponification and surfactant generation.[4] This requires a pH >10 though. Definitive statements on the resulting net effect require further scrutiny.

Kinetics of the LSF Effect. Looking at the time scale of wettability alteration, it is observed that the decrease of the contact angle is slow, even slower than observed for clay substrates or sandstones.[1] Unlike clay substrates, where oil detachment was observed generally under 100 h, in this study, oil detachment is barely observed, even after 150 h. There are potential factors, such as differences in clay and carbonate concentration and coverage at the surface. The carbonate concentration in the suspension was almost 20 times higher than the clay concentration (8000 versus 400 mg/L) used for making patches. With the much smaller clay particles, a fully covered patch can be achieved more easily than with the much coarser carbonate particles. The other contributing factor is the film thickness. In sandstones, it is argued that there is a water film in the thin gap between the oil and clay layer, and this layer can expand at lower salinity conditions because of double-layer expansion, which drives reduction of the contact angle between the oil and rock surface and, subsequently, oil detachment. Slow kinetics was postulated to be related to slow contact (film) diffusion and the presence of pinning points. In carbonates, this film can be unstable though and can rupture because oil (negatively charged) and carbonate (positively charged) can electrostatically bind. Therefore, the water film thickness can be much thinner than in sandstone. Ion diffusion to the film could therefore be much slower, which could also affect the process of the LSE. Needless to say, a further study is required to unambiguously substantiate many of the assumptions made above.

CONCLUSION

The main conclusions from this study are as follows: (1) There is a LSE in carbonates. SW and diluted SW cause wettability change reflected in a contact angle decrease to a more water-wet state. (2) The effect is present even in the absence of mineral dissolution. SW, being unable to dissolve calcite, and diluted SW, equilibrated with calcite, were able to change the wettability of limestone. This is important because, if the effect was entirely related to dissolution, it would not be suited for field applications. (3) These observed changes in contact angle are consistent with the measured changes in ζ-potential from positive to more negative. A wettability change was only observed when the ζ-potential of the oil and carbonate surfaces in our low-salinity brines was lower than the ζ-potential in FW. Consequently, we conclude that a change in surface charge drives the change in carbonate rock wettability and, therefore, the LSF effect. (4) Rock dissolution (of, e.g., calcite and dolomite) may enhance the LSF effect as a secondary mechanism. However, this mechanism is only relevant on a laboratory scale and not a reservoir scale and will lead to an increase in pH. A definitive assessment of the net effect of this pH increase on wettability requires further research. (5) Effect of rock mineralogy: under the same conditions, the magnitude of the LSF effect was smaller for dolomite, i.e., smaller (or no) contact angle change. This could be attributed to stronger adhesion forces between dolomite and oil (on the basis of ζ-potential data) and a smaller response of ζ-potential to lowering salinity. This indicates that a larger reduction of electrostatic charges at the contact line is required to alter wettability of dolomite. (6) The LSF effect is predominantly due to phenomena that occur at the carbonate/brine and carbonate/oil interfaces and to a lesser extent at the oil/brine interface. A mere IFT change with brine salinity cannot explain the observations because (i) IFT reduction is required to trigger a less oil-wetting state, while this is not the case in all brines used in the study, e.g., 25dSW versus SW, (ii) IFT change with the brines that showed an effect is rather small (within 3−4 mN/m), (iii) three-phase contact line is pinned at the carbonate surface because of strong adhesion forces between oil and rock (small changes in IFT cannot move the contact line), and (iv) different responses between dolomite and limestone to the same brine, which indicates that rock plays an important role.

ASSOCIATED CONTENT

Supporting Information

Example of the PHREEQC input file for calculation of equilibrium composition and pH of SW with calcite particles (Appendix 1) and change of Ca^{2+} and Mg^{2+} concentrations in SW and 25dSW after equilibration with either dolomite or

DOI: 10.1021/ef5023847
Energy Fuels 2015, 29, 1352−1367

limestone particles (Appendix 2). This material is available free of charge via the Internet at http://pubs.acs.org.

AUTHOR INFORMATION

Corresponding Author

*E-mail: h.mahani@shell.com.

Notes

The authors declare no competing financial interest.

ACKNOWLEDGMENTS

The authors thank Axel Makurat, Rock and Fluid Science team leader, for providing support to execute this study. The authors are very grateful to Alex Schwing and Rob Neiteler from the experimental support team in Rijswijk, Netherlands. The authors thank Herman Kuipers and Cor van Kruijsdijk for a detailed technical review of the paper and helpful suggestions to improve the manuscript. The authors thank Carl van Rijn, Niels Brussee, Sebastiaan Pieterse, Keschma Ganga, Frans Korndorffer, and Tim Kahs for support in the experiments. Last but not least, the authors thank Shell Global Solutions International B.V. for permission to publish this work.

REFERENCES

(1) Mahani, H.; Berg, S.; Ilic, D.; Bartels, W.-B.; Joekar-Niasar, V. Kinetics of low-salinity-flooding effect. *SPE J.* **2015**, *20* (1), 8−20 DOI: 10.2118/165255-PA.

(2) Bernard, G. Effect of floodwater salinity on recovery of oil from cores containing clays. *Proceedings of the SPE California Regional Meeting*; Los Angeles, CA, Oct 26−27, 1967; Paper SPE 1725.

(3) Tang, G.; Morrow, N. R. Effect of temperature, salinity and oil composition on wetting behavior and oil recovery by waterflooding. *SPE Reservoir Eng.* **1996**, *12* (4), 269−276.

(4) McGuire, P. L.; Chatham, J. R.; Paskvan, F. K.; Sommer, D. M.; Carini, F. H. Low salinity oil recovery: An exciting new EOR opportunity for Alaska's north slope. *Proceedings of the SPE Western Regional Meeting*; Irvine, CA, March 30−April 1, 2005; Paper SPE 93903.

(5) Zhang, Y.; Morrow, N. R. Comparison of secondary and tertiary recovery with change in injection brine composition for crude oil/sandstone combinations. *Proceedings of the SPE/DOE Symposium on Improved Oil Recovery*; Tulsa, OK, April 22−26, 2006; Paper SPE 99757.

(6) Lager, A.; Webb, K. J.; Black, C. J. J.; Singleton, M.; Sorbie, K. Low salinity oil recovery—An experimental investigation. *Petrophysics* **2008**, *49* (1), 28−35.

(7) Agbalaka, C. C.; Dandekar, A. Y.; Patil, S. L.; Khataniar, S.; Hemsath, J. R. Coreflooding studies to evaluate the impact of salinity and wettability on oil recovery efficiency. *Transp. Porous Media* **2009**, *76*, 77−94.

(8) Boussour, S.; Cissokho, M.; Cordier, P.; Bertin, H.; Hamon, G. Oil recovery by low salinity brine injection: Laboratory results on outcrop and reservoir cores. *Proceedings of the SPE Annual Technical Conference and Exhibition*; New Orleans, LA, Oct 4−7, 2009; Paper SPE 124277.

(9) Ligthelm, D. J.; Gronsveld, J.; Hofman, J. P.; Brussee, N. J.; Marcelis, F.; van der Linde, H. Novel waterflooding strategy by manipulation of injection brine composition. *Proceedings of the EUROPEC/EAGE Conference and Exhibition*; Amsterdam, Netherlands, June 8−11, 2009; Paper SPE 119835.

(10) Austad, T.; RezaeiDoust, A.; Puntervold, T. Chemical mechanism of low salinity water flooding in sandstone reservoirs. *Proceedings of the SPE Improved Oil Recovery Symposium*; Tulsa, OK, April 24−28, 2010; Paper SPE 129767.

(11) Hughes, D.; Larsen, S.; Wright, R. *Review of Low Salinity Flooding*; Senergy: Aberdeen, U.K., 2010; Senergy Report Conducted for British Department of Energy and Climate Change (DECC), Document A10DEC015A.

(12) Lee, S. Y.; Webb, K. Y.; Collins, I. R.; Lager, A.; Clarke, S.; O'Sullivan, M.; Routh, A.; Wang, X. Low-salinity oil recovery—Increasing understanding of the underlying mechanisms. *Proceedings of the SPE Improved Oil Recovery Symposium*; Tulsa, OK, April 24−28, 2010; Paper SPE 129722.

(13) Vledder, P.; Fonseca, J. C.; Wells, T.; Gonzalez, I.; Ligthelm, D. Low salinity flooding: Proof of wettability alteration on a field wide scale. *Proceedings of the SPE Improved Oil Recovery Symposium*; Tulsa, OK, April 24−28, 2010; Paper SPE 129564.

(14) Berg, S.; Cense, A. W.; Jansen, E.; Bakker, K. Direct experimental evidence of wettability modification by low salinity. *Petrophysics* **2010**, *51*, 314−322.

(15) Hassenkam, T.; Pedersen, C. S.; Dalby, K.; Austad, T.; Stipp, S. L. S. Pore scale observation of low salinity effects on outcrop and oil reservoir sandstone. *Colloids Surf., A* **2011**, *390*, 179−188.

(16) Mahani, H.; Sorop, T. G.; Ligthelm, D.; Brooks, A. D.; Vledder, P.; Mozahem, F.; Ali, Y. Analysis of field responses to low-salinity waterflooding in secondary and tertiary mode in Syria. *Proceedings of the SPE EUROPEC/EAGE Annual Conference and Exhibition*; Vienna, Austria, May 23−26, 2011; Paper SPE 142960.

(17) Suijkerbuijk, B. M. J. M.; Hofman, J. P.; Ligthelm, D. J.; Romanuka, J.; Brussee, N.; Van der Linde, H. A.; Marcelis, A. H. M. Fundamental investigations into wettability and low salinity flooding by parameter isolation. *Proceedings of the 18th SPE IOR Symposium*; Tulsa, OK, April 14−18, 2012; Paper SPE 154204.

(18) Nasralla, R. A.; Bataweel, M. A.; Nasr-El-Din, H. A. Investigation of wettability alteration and oil-recovery improvement by low-salinity water in sandstone rock. *J. Can. Pet. Technol.* **2013**, *52*, 144−154 DOI: 10.2118/146322-PA.

(19) Fathi, S. J.; Austad, T.; Strand, S. Water-based enhanced oil recovery (EOR) by "smart water" in carbonate reservoirs. *Proceedings of the SPE EOR Conference at Oil and Gas West Asia*; Muscat, Oman, April 16−18, 2012; Paper SPE 154570.

(20) Heberling, F.; Trainor, T. P.; Lutzenkirchen, J.; Eng, P.; Denecke, M. A.; Bosbach, D. Structure and reactivity of the calcite−water interface. *J. Colloid Interface Sci.* **2010**, *354*, 843−857.

(21) Chandrasekhar, S.; Mohanty, K. K. Wettability alteration with brine composition in high temperature carbonate reservoirs. *Proceedings of the SPE Annual Technical Conference and Exhibition*; New Orleans, LA, Sept 30−Oct 2, 2013; Paper SPE 166280.

(22) Yousef, A. A.; Al-Saleh, S.; Al-Jawfi, M. S. Improved/enhanced oil recovery from carbonate reservoirs by tuning injection water salinity and ionic content. *Proceedings of the SPE Improved Oil Recovery Symposium*; Tulsa, OK, April 14−18, 2012; Paper SPE 154076.

(23) Tweheyo, M. T.; Zhang, P.; Austad, T. The effects of temperature and potential determining ions present in seawater on oil recovery from fractured carbonates. *Proceedings of the SPE/DOE Symposium on Improved Oil Recovery*; Tulsa, OK, April 22−26, 2006; Paper SPE 99438.

(24) Rezaei-Gomari, K. A.; Karoussi, O.; Hamouda, A. Mechanistic study of interaction between water and carbonate rocks for enhancing oil recovery. *Proceedings of the SPE EUROPEC/EAGE Annual Conference and Exhibition*; Vienna, Austria, June 12−15, 2006; Paper SPE 99628.

(25) Austad, T.; Strand, S.; Høgnesen, E. J.; Zhang, P. Seawater as IOR fluid in fractured chalk. *Proceedings of the SPE International Symposium on Oilfield Chemistry*; The Woodlands, TX, Feb 2−4, 2005; Paper SPE 93000.

(26) Zhang, P.; Austad, T. Wettability and oil recovery from carbonates: Effects of temperature and potential determining ions. *Colloids Surf., A* **2006**, *279*, 179−187.

(27) Strand, S.; Høgnesen, E. J.; Austad, T. Wettability alteration of carbonates—Effects of potential determining ions (Ca^{2+} and SO_4^{2-}) and temperature. *Colloids Surf., A* **2006**, *275* (1−3), 1−10.

(28) Zhang, P.; Tweheyo, M. T.; Austad, T. Wettability alteration and improved oil recovery by spontaneous imbibition of seawater in

DOI: 10.1021/ef5023847
Energy Fuels 2015, 29, 1352−1367

chalk: Impact of potential determining ions Ca^{2+}, Mg^{2+}, and SO_4^{2-}. *Colloids Surf., A* **2007**, *301*, 199−208.
(29) Webb, K. J.; Black, C. J. J.; Tjetland, G. A laboratory study investigating methods for improved oil recovery in carbonates. *Proceedings of the International Petroleum Technology Conference*; Doha, Qatar, 2005; Paper IPTC 10506.
(30) Romanuka, J.; Hofman, J.; Ligthelm, D. J.; Suijkerbuijk, B. M. J. M.; Marcelis, A. H. M.; Oedai, S.; Brussee, N. J.; Van der Linde, H. A.; Aksulu, H.; Austad, T. Low salinity EOR in carbonates. *Proceedings of the SPE Improved Oil Recovery Symposium*; Tulsa, OK, April 14−18, 2012; Paper SPE 153869.
(31) Gupta, R.; Smith, P. G.; Hu, L.; Willingham, T. W.; Cascio, M. L.; Shyeh J. J.; Harris, C. R. Enhanced waterflood for Middle East carbonate cores—Impact of injection water composition. *Proceedings of the SPE Middle East Oil and Gas Show and Conference*; Manama, Bahrain, Sept 25−28, 2011; Paper SPE 142668.
(32) Zhang, Y.; Sarma, H. Improving waterflood recovery efficiency in carbonate reservoirs through salinity variation and ionic exchanges. *Proceedings of the Abu Dhabi International Petroleum Conference and Exhibition*; Abu Dhabi, United Arab Emirates, Nov 11−14, 2012; Paper SPE 161631.
(33) Alameri, W.; Teklu, T. W.; Graves, R. M.; Kazemi, H.; AlSumaiti, A. M. Wettability alteration during low-salinity water-flooding in carbonate reservoir cores. *Proceedings of the SPE Asia Pacific Oil & Gas Conference and Exhibition*; Adelaide, Australia, Oct 14−16, 2014; Paper SPE 171529.
(34) Shehata, A. M.; Alotaibi, M. B.; Nasr-El-Din, H. A. Waterflooding in carbonate reservoirs: Does the salinity matter? *SPE Reservoir Eval. Eng.* **2014**, 304−313.
(35) Karoussi, O.; Hamouda, A. A. Imbibition of sulfate and magnesium ions into carbonate rocks at elevated temperatures and their influence on wettability alteration and oil recovery. *Energy Fuels* **2007**, *21*, 2138−2146.
(36) Al-Attar, H. H.; Mahmoud, M. Y.; Zekri, A. Y.; Almehaideb, R.; Ghannam, M. Low-salinity flooding in a selected carbonate reservoir: Experimental approach. *J. Pet. Explor. Prod. Technol.* **2013**, *3*, 139−149.
(37) Yousef, A. A.; Al-Saleh, S.; A-Kaabi, A.; AL-Jawfi, M. Laboratory investigation of the impact of injection-water salinity and ionic content on oil recovery from carbonate reservoirs. *SPE Reservoir Eval. Eng.* **2011**, *14* (5), 578−593.
(38) Alotaibi, M. B.; Nasralla, R. A.; Nasr-El-Din, H. A. Wettability challenges in carbonate reservoirs. *Proceedings of the SPE Improved Oil Recovery Symposium*; Tulsa, OK, April 24−28, 2010; Paper SPE 129972.
(39) Zahid, A.; Shapiro, A.; Skauge, A. Experimental studies of low salinity water flooding in carbonate reservoirs: A new promising approach. *Proceedings of the SPE EOR Conference at Oil and Gas West Asia*; Muscat, Oman, April 16−18, 2012; Paper SPE 155625.
(40) Nasralla, R. A.; Sergienko, E.; Masalmeh, S. M.; van der Linde, H. A.; Brussee, N. J.; Mahani, H.; Suijkerbuijk, B. M. J. M.; Al-Qarshubi, I. S. M. Demonstrating the potential of low-salinity waterflood to improve oil recovery in carbonate reservoirs by qualitative coreflood. *Proceedings of the Abu Dhabi International Petroleum Exhibition and Conference*; Abu Dhabi, United Arab Emirates, Nov 10−13, 2014; Paper SPE 172010.
(41) Fernø, M. A.; Grønsdal, R.; Åsheim, J.; Nyheim, A.; Berge, M.; Graue, A. Use of sulfate for water based enhanced oil recovery during spontaneous imbibition in chalk. *Energy Fuels* **2011**, *25*, 1697−1706.
(42) Hiorth, A.; Cathles, L.; Madland, M. The impact of pore water chemistry on carbonate surface charge and oil wettability. *Transp. Porous Media* **2010**, *85* (1), 1−21.
(43) Yousef, A. A.; Al-Saleh, S.; Al-Jawfi, M. S. Improved/enhanced oil recovery from carbonate reservoirs by tuning injection water salinity and ionic content. *Proceedings of the SPE Improved Oil Recovery Symposium*; Tulsa, OK, April 14−18, 2012; Paper SPE 154076.
(44) Austad, T.; Shariatpanahi, S. F.; Strand, S.; Black, C. J. J.; Webb, K. J. Conditions for a low salinity enhanced oil recovery (EOR) effect in carbonate oil reservoirs. *Energy Fuels* **2011**, *26* (1), 569−575.
(45) Pu, H.; Xie, X.; Yin, P.; Morrow, N. R. Low Salinity Waterflooding and Mineral Dissolution. *Proceedings of the SPE Annual Technical Conference and Exhibition*; Florence, Italy, Sept 19−22, 2010; Paper SPE 134042.
(46) Brady, P. V.; Krumhansl, J. L.; Mariner, P. E. Surface complexation modeling for improved oil recovery. *Proceedings of the SPE Improved Oil Recovery Symposium*; Tulsa, OK, April 14−18, 2012; Paper SPE 153744.
(47) Brady, P. V.; Krumhansl, J. L. A surface complexation model of oil−brine−sandstone interfaces at 100 °C: Low salinity waterflooding. *J. Pet. Sci. Eng.* **2012**, *81*, 171−176.
(48) Somasundaran, P.; Agar, G. E. The zero point of charge of calcite. *J. Colloid Interface Sci.* **1967**, *24*, 433−440.
(49) Van Cappellen, P.; Charlet, L.; Stumm, W.; Wersin, P. A surface complexation model of the carbonate mineral−aqueous solution interface. *Geochim. Cosmochim. Acta* **1993**, *57*, 3505−3518.
(50) Pokrovsky, O. S.; Schott, J.; Thomas, F. Dolomite surface speciation and reactivity in aquatic systems. *Geochim. Cosmochim. Acta* **1999**, *63*, 3133−3143.
(51) Mielczarski, J. A.; Schott, J.; Pokrovsky, O. S. Surface speciation of dolomite and calcite in aqueous solutions. In *Encyclopedia of Surface and Colliod Science*, 2nd ed.; Somasundaran, P., Ed.; CRC Press (Taylor & Francis Group): Boca Raton, FL, 2006; Vol. *8*, pp 5965−5978.
(52) Wolthers, M.; Charlet, L.; Van Cappelen, P. The surface chemistry of divalent metal carbonate minerals, a critical assessment of surface charge and potential data using the charge distribution multi-site ion complexation model. *Am. J. Sci.* **2008**, *308*, 905−941.
(53) Alotaibi, M. B.; Nasr-El-Din, H. A.; Fletcher, J. J. Electrokinetics of limestone and dolomite rock particles. *SPE Reservoir Eval. Eng.* **2011**, *14* (5), 594−603.
(54) Zaretskiy, Y., Towards modelling physical and chemical effects during wettability alteration in carbonates at pore and continuum scales. Ph.D. Thesis, Herriot-Watt University, Edinburgh, U.K., 2012.
(55) Morrow, N. R.; Lim, H. T.; Ward, J. S. Effect of crude-oil induced wettability change on oil recovery. *SPE Form. Eval.* **1986**, *1* (1), 89−103.
(56) Hirasaki, G. J. Wettability: Fundamentals and surface forces. *SPE Form. Eval.* **1991**, *6* (2), 217−226.
(57) Kovscek, A. R.; Wong, H.; Radke, C. J. A pore level scenario for the development of mixed wettability in oil reservoirs. *AIChE J.* **1993**, *39* (6), 1072−1085.
(58) Huygens, R. J. M.; Boersma, D. M.; Ronde, H.; Hagoort, J. Interfacial tension measurement of oil−water−steam systems using image processing techniques. *SPE Adv. Technol. Ser.* **1995**, *3* (I), 129−138.
(59) Buckley, J.; Fan, T. Crude oil/brine interfacial tensions. *Petrophysics* **2007**, *48* (3), 175−185.
(60) Morrow, N. R. The effects of surface roughness on contact angle with special reference to petroleum recovery. *J. Can. Pet. Technol.* **1975**, *14* (04), 42−53.
(61) McCormack, D.; Carnie, S. L.; Chan, D. Y. C. Calculations of electric double-layer force and interaction free energy between dissimilar surfaces. *J. Colloid Interface Sci.* **1995**, *169*, 177−196.
(62) Compton, R. G.; Daly, P. J. The dissolution kinetics of Iceland spar single crystals. *J. Colloid Interface Sci.* **1984**, *101* (1), 159−166.
(63) Wallin, M.; Bjerle, I. Rate models for limestone dissolution: A comparison. *Geochim. Cosmochim. Acta* **1989**, *53*, 1171−1176.
(64) Kim, T. W.; Kovscek, A. R. Wettability alteration of a heavy oil/brine/carbonate system with temperature. *Energy Fuels* **2013**, *27* (6), 2984−2998.

DOI: 10.1021/ef5023847
Energy Fuels 2015, 29, 1352−1367